Journal of Power Sources 359 (2017) 441–449

Contents lists available at ScienceDirect

Journal of Power Sources

journal homepage: www.elsevier.com/locate/jpowsour

Highly conductive solid polymer electrolyte membranes based on polyethylene glycol-*bis*-carbamate dimethacrylate networks

Guopeng Fu [a], Janel Dempsey [a, b], Kosuke Izaki [a, c], Kaoru Adachi [c], Yasuhisa Tsukahara [c], Thein Kyu [a, *]

[a] Department of Polymer Engineering, University of Akron, Akron, OH 44325, United States
[b] Chemistry Department, John Carroll University, University Heights, OH 44118, United States
[c] Department of Chemistry and Materials Technology, Kyoto Institute of Technology, Kyoto 606-8585, Japan

HIGHLIGHTS

- As-synthesized PEGBDCDMA is thermally stable and mechanically sturdy.
- Room temperature ionic conductivity of our solid PEM reaches 10^{-3} S/cm.
- The present solid PEM exhibits a wide electrochemical stability window.
- High capacity retention has been achieved in charge/discharge cycling tests.

GRAPHICAL ABSTRACT

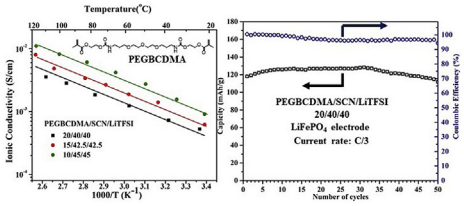

ARTICLE INFO

Article history:
Received 5 April 2017
Received in revised form
24 May 2017
Accepted 28 May 2017
Available online 3 June 2017

Keywords:
Lithium ion battery
Polymer electrolyte membranes
High ionic conductivity

ABSTRACT

In an effort to fabricate highly conductive, stable solid-state polymer electrolyte membranes (PEM), polyethylene glycol *bis*-carbamate (PEGBC) was synthesized via condensation reaction between polyethylene glycol diamine and ethylene carbonate. Subsequently, dimethacrylate groups were chemically attached to both ends of PEGBC to afford polyethylene glycol-*bis*-carbamate dimethacrylate (PEGBCDMA) precursor having crosslinking capability. The melt-mixed ternary mixtures consisting of PEGBCDMA, succinonitrile plasticizer, and lithium trifluorosulphonyl imide salt were completely miscible in a wide compositional range. Upon photo-crosslinking, the neat PEGBCDMA network was completely amorphous exhibiting higher tensile strength, modulus, and extensibility relative to polyethylene glycol diacrylate (PEGDA) counterpart. Likewise, the succinonitrile-plasticized PEM network containing PEGBCDMA remained completely amorphous and transparent upon photo-crosslinking, showing superionic conductivity, improved thermal stability, and superior tensile properties with improved capacity retention during charge/discharge cycling as compared to the PEGDA-based PEM.

1. Introduction

Lithium-ion batteries have gained increasing recognition due to their wide variety of applications including electric vehicles, electronics, and implantable medical devices [1–4]. Most lithium-ion batteries in use today consist of a lithium salt dissolved in a mixture of cyclic/acyclic organic carbonate solvents, capable of facilitating fast diffusion of lithium ions [5]. However, these mixed organic liquids, being volatile and flammable by virtue of their low flash points and poor thermal management, have resulted in battery explosion and catching fires [6,7]. One strategy is to replace the volatile carbonate solvent with a nonvolatile, solid electrolyte system that allows for fast ion movement and also binds well with

* Corresponding author.
E-mail address: tkyu@uakron.edu (T. Kyu).

http://dx.doi.org/10.1016/j.jpowsour.2017.05.097
0378-7753/

the electrodes [8,9]. Wright and co-workers reported that the ether-based polymer, viz., polyethylene oxide (PEO) was capable of dissolving inorganic salts and thus afforded ion conduction, albeit low [10,11]. Some recent works have shown that doping a plastic crystal such as succinonitrile (SCN) into a polymer electrolyte membrane (PEM) can achieve a high ionic conductivity in excess of 10^{-3} S/cm [12–14]. The feasibility of producing solvent-free solid electrolyte was demonstrated by utilizing PEO as matrix and doping with SCN plastic crystals for lithium ion transport. It was found that this polymer electrolyte achieved reasonably high ionic conductivity in the order of 10^{-4} S/cm at room temperature, despite the fact that SCN itself is a poor ionic conductor. However, such PEO based PEM containing lithium salt (LiTFSI) is a waxy substance without sustainable mechanical strength or integrity, thereby preventing its full utilization as solid electrolyte [15,16]. Upon replacing PEO with photo-curable poly(ethylene glycol) diacrylate (PEGDA), the tensile strength of the photo-cured PEM has improved to 0.10 MPa while the network plasticization by SCN expedites the lithium ion transport [17–19].

In solid-state battery applications, the performance of the PEM depends not only on their electrochemical properties, but also on their mechanical properties such as tensile strength, modulus, and elongation at break. During the repeated charge/discharge cycling of the conventional liquid electrolyte battery, lithium dendrite was found to grow on the negative electrode, which eventually reached the cathode resulting in short-circuiting, thereby compromising safety [20]. Such dendrite growth may be prevented by using mechanically tougher PEM without compromising high ionic conductivity [21,22]. Photopolymerized polyethylene glycol diacrylate (PEGDA) networks have shown improved mechanical strength and modulus while imparting flame retardant property and chemical stability to the solid PEM. However, room temperature ionic conductivity of neat PEGDA based binary PEMs is inherently low and thus plasticization of these PEM networks is desirable to reach the level of superionic conductivity, viz., $>10^{-3}$ S/cm. It was demonstrated that small-molecule plasticizers such as succinonitrile (SCN) can boost not only ionic conductivity, but also enhance the dissociation (i.e., ionization) of the lithium salt in the solid-state polymer electrolyte membranes.

In this paper, polyethylene glycol (PEG) containing telechelic amine groups were end-linked with cyclic ethylene carbonate via ring-opening reaction to afford polyethylene glycol *bis*-carbamate (PEGBC). Subsequently, UV-curable methacrylate groups were further attached at both chain ends to form polyethylene glycol-*bis*-carbamate dimethacrylate (PEGBCDMA) to impart crosslinking capability. By virtue of the low glass transition, the urethane segments in PEGBC further promotes the ionic conductivity, while the photo-cured PEGBCDMA has achieved high tensile strength, modulus, and extensibility. Of particular interest is that the electrochemical performance including high ionic conductivity and capacity retention with improved thermal stability has been achieved with the present PEGBCDMA based solid PEMs.

2. Experimental section

Materials. Lithium bis(trifluoromethane) sulfonimide (LiTFSI) having a purity of 99.9%, succinonitrile (SCN) (>99%), ethylene carbonate (EC, 99%), 4,7,10-trioxa-1,13-tridecanediamine (TTDDA, 97%, also known as PEG diamine), 4-(dimethyl-amino) pyridine (DMAP, 99%), hydroquinone (99%), triethyleneamine (TEA, 99%) and methacrylic anhydride (MAA, 94%) were purchased from Sigma-Aldrich Co. The solvents such as dichloromethane (99.9%), methylene chloride (99.9%) and acetone (99.9%) were bought from Fisher Scientific Co. The electrode materials $LiFePO_4$, $Li_4Ti_5O_{12}$ and acetylene black powders were purchased from MTI Corp. Poly (vinylidene fluoride) (PVDF having Mw ~534,000) binder and 1-methyl-2-pyrrolidinone (NMP) solvent were obtained from Sigma-Aldrich.

Sample Preparation. The LiTFSI salt was dried at 170 °C under vacuum for 24 h before blending. Varying weight percentages of PEGBC and LiTFSI mixtures were prepared by dissolving in the mixed dichloromethane/acetone (40/1 w/w) solvent in a nitrogen-purged glove box. Solution casting of the blend solution was carried out at 80 °C for under continuous nitrogen flow. Subsequently, these PEGBC/LiTFSI blends were further dried at 150 °C in a vacuum oven for 12 h.

In the fabrication of solid PEM films, several compositions of PEGBCDMA/SCN/LiTFSI were selected that correspond to the isotropic region of the ternary phase diagram (figure not included). Melt-mixing was performed at room temperature by mechanically stirring without using any solvent. 2 wt% of Irgacure 819® with respect to the PEGBCDMA amount was added to the above mixtures during melt mixing. The homogeneous mixture thus obtained was placed on a glass slide within a tape frame spacer having a square shape with a dimension of 10 × 10 mm^2, and then covered with a transparent cover glass. Subsequently, UV polymerization was performed at room temperature (25 °C) by illuminating with a UV Cure Lamp (Bondwand 350 nm) at an intensity of 5 $mWcm^{-2}$ for 15 min in a glove box under nitrogen atmosphere. The thickness of the photocured transparent film was approximately 0.2 mm.

For electrochemical measurements, the working electrodes were prepared by mixing active materials (lithium iron phosphate ($LiFePO_4$) or lithium titanium oxide ($Li_4Ti_5O_{12}$)), acetylene black, and polyvinylidene fluoride (PVDF) polymer binder in NMP solvent at a weight ratio of 8:1:1. The slurry mixture was coated onto stainless steel and current collectors such as aluminum or copper foil, and then dried at 160 °C in vacuum for 24 h. The coin-cell batteries were assembled in half-cell configurations using a lithium metal foil (Alfa Aesar Co.) as the counter (or reference) electrode in an argon gas-filled glovebox. In the battery assembling process, the polymer electrolyte membrane was placed on top of the electrode by applying a very light pressure to improve the contact between the cathode and PEM.

Sample characterization. Thermal properties of the samples were examined using a thermogravimetric analyzer (TGA; Model Q50, TA Instruments) at a heating rate of 10 °C/min from room temperature to 600 °C under a nitrogen atmosphere. The glass transition temperatures of the PEM samples were determined using differential scanning calorimetry (DSC) (Model Q200, TA Instruments) in which the blend samples weighing 5 mg were hermetically sealed with aluminum lids in a glovebox under nitrogen to alleviate moisture absorption. All DSC scans were acquired at a ramp rate of 10 °C/min unless indicated otherwise. Fourier transform infrared (FTIR) spectra were acquired by means of an FTIR spectrometer (Alpha-P, Bruker Optics) in a transmission mode. The tensile properties of neat polymer matrices were evaluated using a tensile tester (Model 5900, Instron) at a constant displacement rate of 10 mm/min. The typical size of all the samples for the tensile test was 4 × 10 mm^2 and the film thickness was approximately 1 mm. For softer plasticized PEM films, tensile measurements were performed using a dynamic mechanical analyzer (DMA Q800 TA instruments) at a constant stress rate of 0.1 MPa/min. All tensile tests were conducted at ambient temperature.

Ionic conductivities were determined by using an AC impedance analyzer (HP4192A LF, Hewlett Packard). Samples were sealed between two parallel stainless steel polished plates with an area of 10 × 10 cm^2 and ~0.2 mm in thickness. Sample loading was undertaken in a glovebox to prevent moisture absorption, if any. The frequency sweep was carried out from 13 MHz to 5 Hz with a

voltage of 10 mV in amplitude. Temperature ramping was performed in a heating chamber for all PEMs at a rate of 1 °C/min. Cyclic voltammetry measurements were undertaken by using SI 1260 Impedance/Gain Phase Analyzer in conjunction with SI 1287 Electrochemical Interface (Solartron Analytical Inc.). Coin cells were assembled in the stainless steel (SS)/PEM/Li configuration. The operating voltage range was from −0.5–6.0 V with a scan rate of 1 mV/s. Galvanostatic charge/discharge cycling tests of the aforementioned half-cells were conducting using MTI 8-channel battery cycler (MTI Corp.). The operation voltages for the $LiFePO_4$/PEM/Li and $Li_4Ti_5O_{12}$/PEM/Li cells were in the ranges of 2.5–4.2 V and 1.0–2.5 V, respectively.

3. Results and discussion

3.1. Synthesis and characterization of PEGBC

In the fabrication of highly conductive, stable solid-state polymer electrolyte membranes (PEM), polyethylene glycol-*bis*-carbamate (PEGBC, Scheme 1) was synthesized via a ring-opening reaction of ethylene carbonate and 4,7,10-trioxa-1,13-tridecanediamine (TTDDA; commonly known as polyethylene glycol diamine (PEG diamine)) [23]. In a typical procedure of PEGBC preparation, ethylene carbonate (8.81 g, 0.10 mol) was first dissolved in 50 mL dichloromethane. Subsequently, the above solution was added drop-wise into the TTDDA (11.00 g, 0.05 mol) and dichloromethane (50 mL) mixture in ice water bath and then the mixture was stirred at room temperature for 24 h. A slightly yellow liquid with a yield of 82% was obtained after evaporation of dichloromethane.

The IR spectrum of the resulting PEGBC was acquired to compare with the IR spectra of the starting PEG diamine (see the chemical structure of TTDDA in Scheme 1) and EC (see Fig. 1). While there are several interesting features reflecting the differences in chemical structures of the constituent molecules, we shall focus our attention on the O–H (3300–3400 cm^{-1}), N–H (at 3370 cm^{-1}) and C=O (1650–1800 cm^{-1}) stretching bands. The broad peak in the spectrum in the vicinity of 3300–3400 cm^{-1} is an overlap of O–H stretching of a diol unit (i.e., glycol at 3327 cm^{-1}) and N–H stretching (at 3371 cm^{-1}) of PEGBC. According to Scheme 1, one can witness the formation of hydroxyl group during the ring opening reaction between EC and the amine group of the PEG-diamine affording *bis*-carbamate (or urethane diol), which was evidently absent in the spectra of neat EC and of neat PEG diamine. The drastic shift of wavenumber of the carbonyl stretching (from 1769 cm^{-1} belonging to carbonate group of EC to 1691 cm^{-1} of C=O of urethane) and the O–H stretching at 3327 cm^{-1} of the hydroxyl end-groups suggests the possible hydrogen bonding between the amide group of PEGBC and the O–H terminal groups (see Scheme 1). The peak at 1691 cm^{-1} may be attributed to the carbonyl unit belonging to urethane group of PEGBC. Additionally, the appearance of new amide bands at 1529 and 1258 cm^{-1} suggests the formation of urethane linkages in the PEGBC.

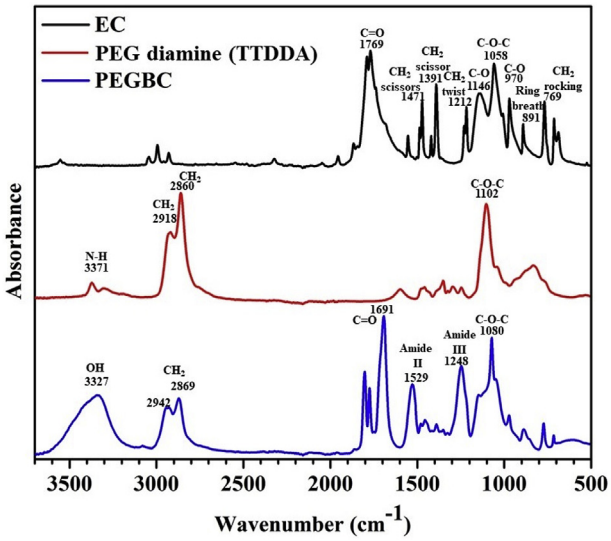

Fig. 1. Infrared spectra of PEG diamine, EC and PEGBC showing characteristic bands along with the corresponding assignments.

Differential scanning calorimetry (DSC) study was undertaken to examine the thermal behavior of binary mixtures of PEGBC and LiTFSI. Fig. 2(a) exhibits the variation of DSC thermograms as a function of blend composition of the PEGBC/LiTFSI mixtures. The neat PEGBC as well as its blends with LiTFSI show a single glass transition (T_g) with an overshoot in the transition zone of T_g. Such T_g overshoot can be discerned not only in the neat PEGBC, but also in the PEGBC-rich compositions, which is commonly observed in polyamide [24,25]. More importantly, the single T_g moves systematically to higher temperatures from −47.3 to −17 °C with increasing amount of LiTFSI from 0 (neat PEGBC) to 90% (10/90). It is well known that ethylene carbonate is not only as an excellent plasticizer to electrolytes, but also known for its ionizing capability to the lithium salt. Hence, the present carbamate group of PEGBC chain is anticipated to effectively dissociate the lithium ions (or ionize the salt) and possibly plasticization of the ion-dipole complexes. The revelation of single glass transition combined with the systematic movement with composition suggests the miscible character of these blends, although by no means a proof. These blends are transparent and show gel-like appearance. The increase in the T_g from −47.3 to −17 °C with increasing LiTFSI concentration implies the stiffening of the PEGBC chains and/or formation of ionic gels (or temporary networks) driven by the strong complexation between the dissociated Li cations with ether oxygen of PEG as well as C=O of urethane groups. The T_g enhancement suggests that the ion-dipole complexation predominates over the plasticization effect afforded by the carbamate. It is reasonable to infer that the chain stiffening and/or the formation of gel-like networks driven by

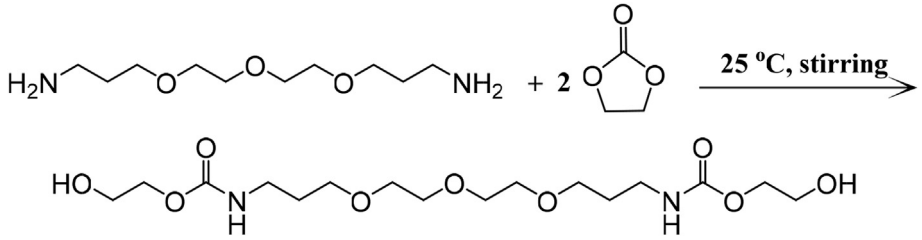

Scheme 1. Synthesis scheme of polyethylene glycol-*bis*-carbamate (PEGBC) from poly(ethylene glycol) diamine (TTDDA, i.e., PEG diamine) and 2 equivalents of ethylene carbonate (EC) via ring-opening reaction.

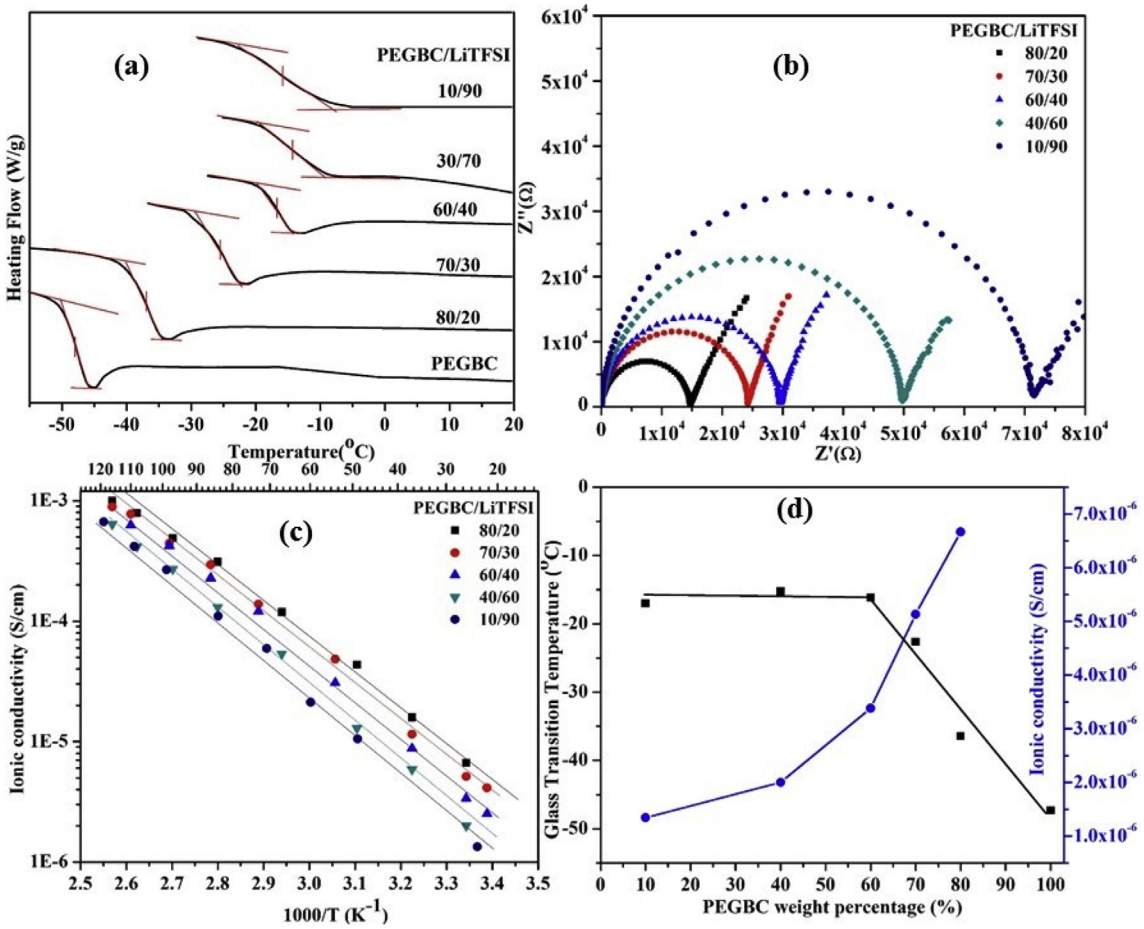

Fig. 2. (a) DSC thermograms of PEGBC and LiTFSI mixtures; (b) Nyquist plots of PEGBC/LiTFSI mixtures with various concentration measured at 25 °C; (c) The Arrhenius plots of ionic conductivity versus reciprocal temperature at various compositions; (d) Variation of glass transition temperature and ionic conductivity as a function of PEGBC contents of binary PEGBC/LiTFSI mixtures.

the strong ion-dipole interaction has contributed to the drastic increase of the T_g of PEGBC chains upon complexation with the surrounding Li cations.

In an effort to determine the ion transport behavior, the complex impedance in the compliance form, i.e. ($Z^* = Z' - iZ''$), was determined by means of AC impedance spectroscopy. Fig. 2(b) shows the Cole-Cole plot (alternatively known as Nyquist plot) as a function of blend ratio of PEGBC/LiTFSI, obtained at 25 °C. As manifested by expanding diameters of the Z′ versus Z″ semicircles, the material resistivity to ion transport has risen with increasing concentration of LiTFSI salt in the blends. To better appreciate the conductivity behavior, the AC impedance measurements were performed as a function of temperature. The ionic conductivity of PEGBC/LiTFSI mixtures can be determined from the Nyquist plots in Fig. 2(b). The logarithmic ionic conductivity versus reciprocal absolute temperature plots of all PEGBC/LiTFSI mixtures reveals the linear relationship suggestive of Arrhenius behavior (Fig. 2(c)). Given the parallel slopes of the Arrhenius plots, the same mechanism may be operating for all binary blend compositions with the same apparent activation energy of 24 kJ/mol [19]. The room-temperature ionic conductivity values were plotted as a function of blend composition by comparing with the glass transition temperatures in Fig. 2(d). As can be seen in Fig. 2(a), the glass transition temperature initially remains stationary initially and then it decreases with further increase of PEGBC. The ionic conductivity of the 10/90 PEGBC/LiTFSI binary mixture is rather poor, 1×10^{-6} S/cm, and it continues to increase with increasing polymer content. At LiTFSI rich region, increasing polymer concentration does not affect the T_g, while the ionic conductivity increases at a slower pace. When PEGBC exceed 60 wt%, the drastic increasing ionic conductivity and the declining T_g suggest the possible existence of a strong correlation between the enhanced polymer chain dynamics and lithium ion transport [26,27].

Synthesis polyethylene glycol-*bis*-carbamate dimethacrylate (PEGBCDMA) and characterization of its solid PEM films.

The as-synthesized PEGBC (from Scheme 1) terminated with urethane diol (9.9 g, 0.025mol) was dissolved in 60 mL dichloromethane. The mixture was mixed in a flask and kept in an ice bath. Subsequently, 4-(dimethyl-amino) pyridine (DMAP) catalyst (30.5 mg, 0.25 mmol), and hydroquinone inhibitor (7 mg, 0.0625 mmol) were added, followed by drop-wise addition of triethyleneamine (TEA) (7.0 g, 0.06 mol) and of methacrylic anhydride (9.85 g, 0.06 mol) under the nitrogen atmosphere. The reaction mixture was stirred at approximately 0 °C (i.e., in ice water bath) for 24 h. Then saturated sodium bicarbonate solution (300 g) was added drop-by-drop to obtain a two-phase separated liquid mixture. The product (the bottom layer) was collected, washed with brine (300 mL 3×) and distilled water (300 mL 3×). After the dichloromethane was evaporated, a yellow liquid product was obtained (yield: 43.9%); hereafter denoted polyethylene glycol-*bis*-carbamate dimethacrylate (PEGBCDMA) (Scheme 2).

The FTIR investigation was carried out on the resulting

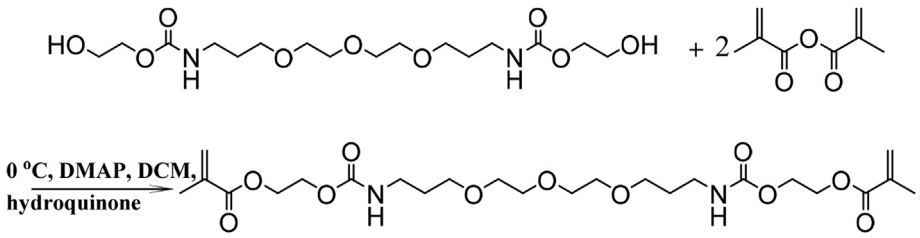

Scheme 2. Synthesis of polyethylene glycol-*bis*-carbamate dimethacrylate (PEGBCDMA) from PEGBC and methacrylic anhydride.

PEGBCDMA. The characteristic absorption peak 3350 cm^{-1} is attributable to N-H stretching vibration. The absorptions at 2945 cm^{-1} and 2868 cm^{-1} correspond to the CH_2 stretching peaks. The peak at 1527 cm^{-1} is related to C–N stretching vibrations in combination with N–H bending (Amide II band). The peak at 1241 cm^{-1} is ascribed to the in-phase combination of N–H in-plane-bending and C–N stretching vibrations (Amide III band) [28–30]. As shown in Fig. 3(a), the O–H stretching band (3500 cm^{-1}) has diminished while appearing like a shoulder on the pronounced N–H stretching peak at 3350 cm^{-1}, suggestive of the reduction of O–H terminal group due to its reaction with methacrylic anhydride.

Subsequently, PEGBCDMA was photo-crosslinked by illuminating with UV light (at 350 nm) for 10 min. The FTIR spectra of cured PEGDA and PEGBCDMA before and after photo-curing were compared in Fig. 3(a). Two characteristic bands at 816 and 1636 cm^{-1} belonging to the C=C stretching and twisting modes before and after photocuring were analyzed by zooming-in Fig. 3(b) and (c). Fig. 3(b) exhibits an enlarged region from 790 to 830 cm^{-1}, where the signal corresponding to the C=C double bonds of acrylate group is clearly reduced which is attributable to the crosslinking. Similarly, Fig. 3(c) shows that the peak of C=C twisting of acrylate group at 1636 cm^{-1} virtually disappears after crosslinking. This evidence suggests that most of the C=C double bonds (i.e., ~89%) in the acrylate end groups have been consumed in the UV crosslinking reaction.

The resulting PEGBCDMA film is transparent to naked eyes and it is completely amorphous as manifested by DSC. As shown in Fig. 4(a), tensile tests were performed on the neat PEGBCDMA network in comparison with those of polyethylene glycol diacrylate (PEGDA) films. Herein, we preferred a low molecular weight PEGDA having M_w of 700 g/mol for comparison since it has comparable molecular weight with that of the as-synthesized PEGBCDMA, which is 528 g/mol. Although PEGDA (700 g/mol) network films exhibited slightly inferior mechanical properties relative to those of a higher molecular weight PEGDA (6000 g/mol) counterpart, the mechanical strength and elongation-at-break of these films are still acceptable for battery assembling and repeated charge/discharge cycling. Moreover, PEGDA (700 g/mol) is available in a large quantity from commercial sources.

According to Fig. 4 (a), the tensile strength of PEGBCDMA film is around 32 MPa and the elongation at break is 55%, whereas the tensile strength of the reference PEGDA film is about 2 MPa with the elongation at break is 18%. Hence, the mechanical strength and toughness of PEGBCDMA networks have significantly surpassed those of the PEGDA films. The enhancement of the mechanical strength and extensibility of PEGBCDMA relative to PEGDA may be attributed to intermolecular hydrogen bondings between amine

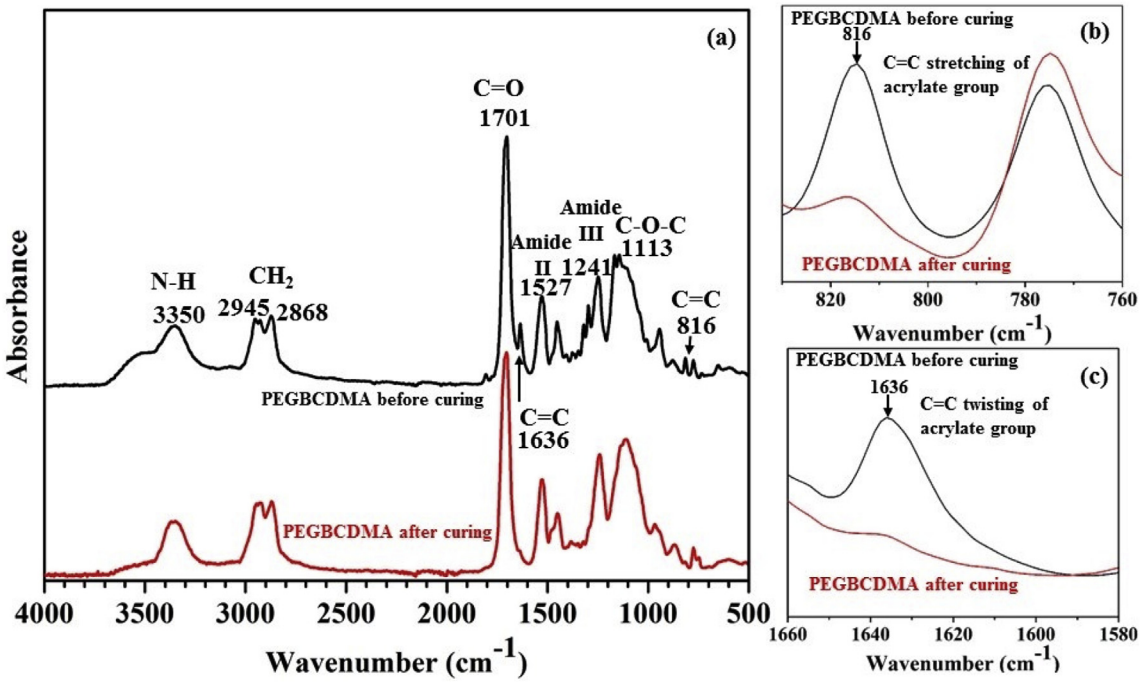

Fig. 3. (a) Infrared spectra of PEGBCDMA before and after polymerization. (b) The enlarged region between 790 and 830 cm^{-1} characteristics of C=C twisting of acrylate group. (c) Zoomed-in region between 1580 and 1660 cm^{-1} corresponding to the C=C stretching of acrylate group.

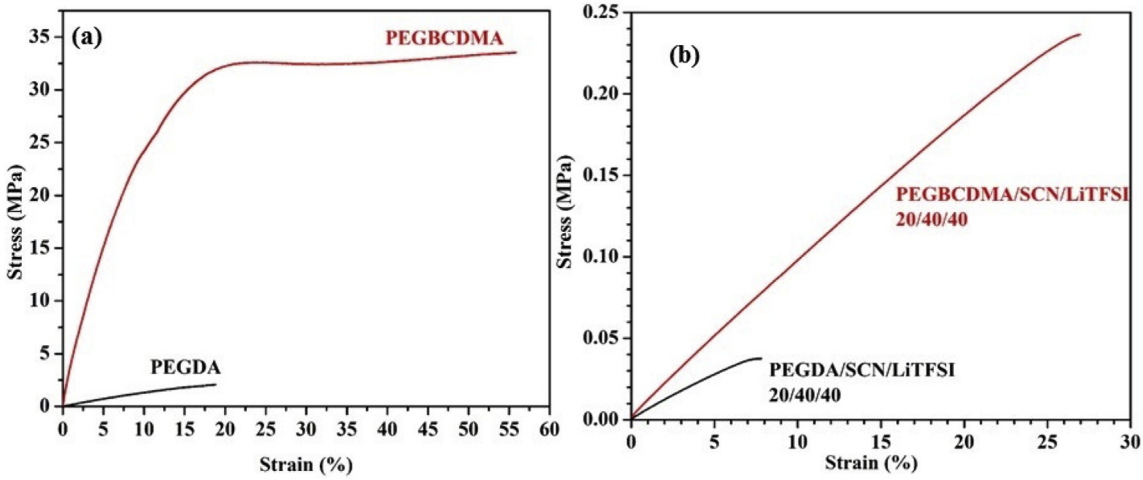

Fig. 4. (a) Comparison of stress-strain behavior of UV-cured neat PEGBCDMA and PEGDA and (b) of photo-cured PEMs with 20/40/40 PEGDA/SCN/LiTFSI and 20/40/40 PEGBCDMA/SCN/LiTFSI.

(N–H) and carbonyl (C=O) and/or amide groups [31,32]. The intermolecular hydrogen bond between the amine group to the carbonyl group of the urethane or the amine group to the carbonyl group from the ester serves as physical crosslinked points in addition the chemical junctions afforded by the crosslinking of the methacrylate bonds. Given the fact that the molecular weight of PEGBCDMA and PEGDA are comparable, it is likely that the urethane linkages in the PEGBCDMA networks may have afforded greater extensibility as manifested in Fig. 4(a).

Similar tensile behavior can be witnessed in their SCN-plasticized PEMs in Fig. 4(b). It should be pointed out that the stress-strain curves of the plasticized PEMs (i.e., 20/40/40 PEGDA/SCN/LiTFSI and 20/40/40 PEGBCDMA/SCN/LiTFSI) exhibit one order of magnitude lower in stress as compared to the unplasticized neat counterparts. The PEM containing PEGBCDMA still reveals a considerably higher tensile strength (~0.24 MPa) relative to that of the PEM containing PEGDA (0.04 MPa), which is consistent with the trend demonstrated in Fig. 4(a) of their neat forms. Of particular importance is that PEM containing PEGBCDMA also has a higher network elasticity, thereby affording a higher elongation at break (~27%), which may be attributed to the flexibility of the urethane linkages in PEGBCDMA chains.

Fig. 5 shows the TGA thermograms of thermogravimetric analysis. The neat ethylene carbonate (EC), being a small molecule, starts to degrade in the vicinity of 80 °C. As expected, the PEGBC derivative shows a better thermal stability up to 240 °C relative to neat EC. Upon crosslinking, the PEGBCDMA network shows greater thermal stability close to 300 °C. By virtue of the improved thermal stability and mechanical properties, the PEGBCDMA network is expected to serve as a better matrix to the solid-state PEM in lithium battery applications.

Next, the ionic conductivity of various plasticized solid PEMs was determined as a function of PEGBCDMA amount while keeping the SCN/LiTFSI ratio constant, viz. 20/40/40, 15/42.5/42.5, and 10/45/45 PEGBCDMA/SCN/LiTFSI. The choice of lesser PEGBCDMA matrix in the PEM formulation is due to the improved mechanical strength and extensibility relative to the PEGDA based PEM. Moreover, it can be anticipated that the lesser the matrix polymer in the PEM, the greater the ionic conductivity. Fig. 6 exhibit ionic

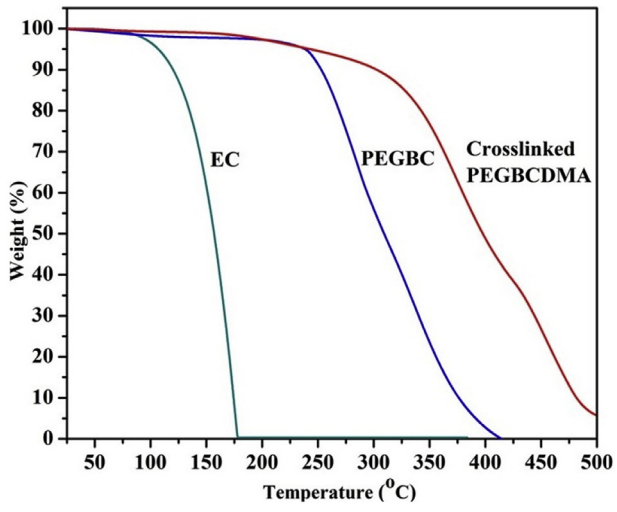

Fig. 5. Comparison of TGA-thermograms of neat EC, PEGBC, and PEGBCDMA, showing improved thermal stability of the photo-crosslinked network.

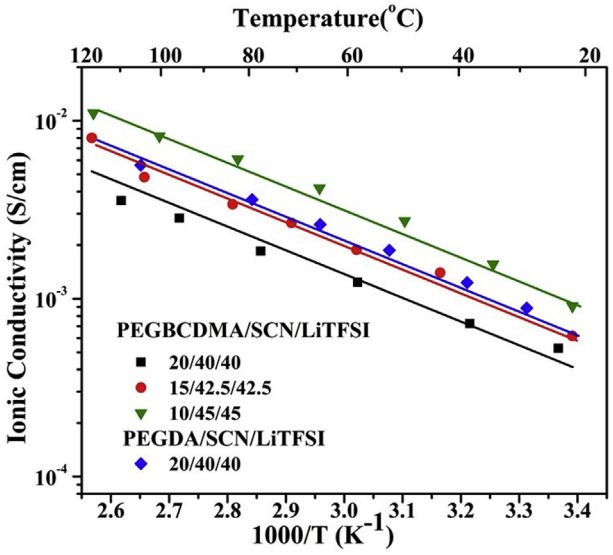

Fig. 6. Arrhenius plots of PEM as a function of PEGBCDMA amount while keeping the SCN/LiTFSI ratio constant in comparison with that of the PEM consisting of 20/40/40 PEGDA/SCN/LiTFSI.

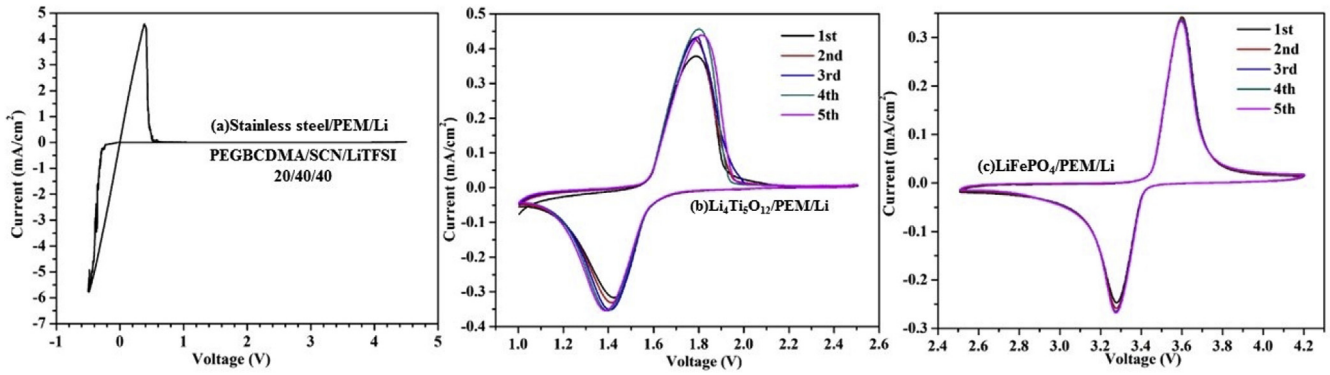

Fig. 7. (a) Cyclic voltammograms for PEGBCDMA/SCN/LiTFSI 20/40/40 PEM, showing the stability up to 4.5 V tested at a scan rate of 1 mV/s. Cyclic voltammograms of the (b) $Li_4Ti_5O_{12}$ and (c) $LiFePO_4$ cathode half-cell versus Li metal electrode at a scan rate 1 mV/s.

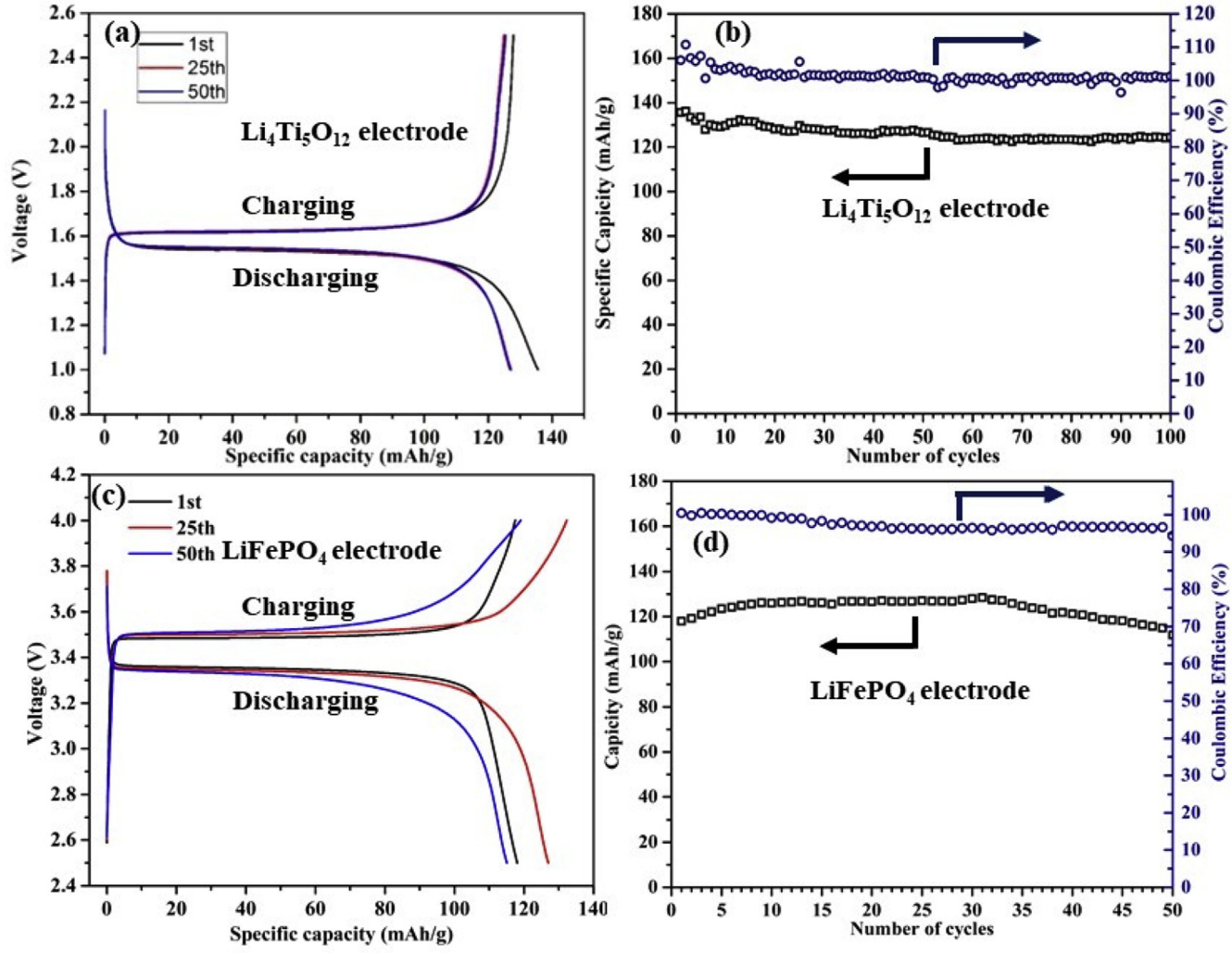

Fig. 8. (a) Voltage as a function of the specific capacity of $Li_4Ti_5O_{12}$/PEM/Li half-cells; (b) Galvanostatic charge-discharge capacity versus cycle number of $Li_4Ti_5O_{12}$/PEM/Li half-cells. (c) Voltage as a function of the specific capacity of $LiFePO_4$/PEM/Li half-cells; (d) Galvanostatic charge-discharge capacity versus cycle number of $LiFePO_4$/PEM/Li half-cells at the current rate of C/3.

conductivity for PEGBCDMA/SCN/LiTFSI polymer electrolyte membrane (PEM) as a function of temperature in accordance with Arrhenius plots for three PEGBCDMA concentrations: 20/40/40, 15/42.5/42.5 and 10/45/45 PEGBCDMA/SCN/LiTFSI. The ionic conductivity of all compositions shows the linear relationship in logarithmic ionic conductivity versus reciprocal absolute temperature plots, suggestive of the Arrhenius character. At the 10% and 15% of PEGBCDMA, the ionic conductivity of PEM has reached the superionic conductivity level of 10^{-3} S/cm at room temperature, which is almost the same as that of the 20/40/40 PEGDA-based

PEM. When temperature increases to 120 °C, the ionic conductivity reaches the order of 10^{-2} S/cm, which is comparable to that of the organic liquid electrolyte, but with significantly improved thermal stability.

Although the 10/45/45 PEGBCDMA/SCN/LiTFSI shows the highest conductivity at both room temperature and a high temperature of 60 °C, the 20/40/40 composition is chosen for the cycling tests by virtue of its better mechanical properties. Despite the slightly lower ionic conductivity, the 20/40/40 PEM is more suitable for battery assembly and also for the charge/discharge cycling tests, since PEMs as well as electrodes can expand and contract leading to cracking and premature failure.

The electrochemical stability of PEM with 20/40/40 PEGBCDMA/SCN/LiTFSI was evaluated by means of cyclic voltammetry (CV). The above PEM was assembled into a coin cell configuration using stainless steel as a working electrode and lithium metal foil as the counter (i.e., reference) electrode. Fig. 7(a) shows the first CV cycle from −0.5 to 4.5 V versus Li/Li^+ at a scanning rate of 1 mV/s. The oxidative stability of the PEM exhibited good electrochemical stability up to about 4.5 V, indicating an electrochemical stability window of PEM from 0.5 to 4.5 V. This wide electrochemical voltage window affords the present PEM as the potential solid electrolyte for the $LiFePO_4$ cathode (2.5–4.2 V) and $Li_4Ti_5O_{12}$ anode (1.0–2.5 V) in the application in solid-state lithium ion battery.

Fig. 7 (b) and (c) show the CV of 20/40/40 PEGBCDMA/SCN/LiTFSI PEM in $Li_4Ti_5O_{12}$ and $LiFePO_4$ cathode half-cell using the Li metal foil as the reference electrode. Fig. 7(b) exhibits the CV curve of the PEM in the half-cell configuration of $Li_4Ti_5O_{12}$ anode against the Li metal electrode in the potential range from 2.5 to 1.0 V (vs. Li/Li^+) at a scan rate of 1 mV/s. The pronounced cathodic peak at 1.8 V and the anodic peak at 1.4 V can be attributed to the redox reaction of Ti^{4+}/Ti^{3+}, respectively, which is associated with lithium insertion/extraction in the spinel $Li_4Ti_5O_{12}$ crystal lattice. In Fig. 7(c) the delithiation process started during increasing voltage from the open circuit voltage (around 2.7 V, data not shown), which corresponds to the cathodic peak at 3.7 V. While the anodic peak at 3.3 V is analogous to the lithiation process. The CV curves in the $LiFePO_4$ cathode and $Li_4Ti_5O_{12}$ anode half-cell are consistent in both shape and size (magnitude) in all five cycles tested, which indicates a good reversibility of the electrochemical reactions within the voltage range investigated.

To evaluate the electrochemical performance of the PEM in lithium ion battery, a $Li/PEM/Li_4Ti_5O_{12}$ prototype half-cell was fabricated using the PEM having 20 wt% PEGBCDMA, 40 wt% SCN and 40 wt% LiTFSI (or labeled as 20/40/40). Fig. 8(a) and (b) presents the charge − discharge profiles of the cell, obtained at a current density 50 mA/g corresponding to a current rate of C/3 with the cut-off voltages between 1.0 V and 2.5 V. Stable voltage plateaus have been observed at 1.63 V corresponding to the Li^+-insertion and 1.55 V for Li^+-desertion (or stripping), respectively [33,34]. The initial capacity was approximately 130 mA h/g with a minor capacity decay (i.e., 95% of the capacity was sustained after 50^{th} cycles), indicating a better stability relative to that of the PEM containing PEGDA (which retained about 80% of the initial capacity after 50 cycles) [35,36]. The Columbic efficiency is virtually invariant at about 100% for 50 cycles tested.

Fig. 8(c) exhibits the corresponding charge–discharge profiles of the $Li/PEM/LiFePO_4$ half-cell obtained at the C/3 rate with a cutoff voltage of 4.0 V for the upper limit and 2.5 V for the lower limit. Voltage plateau corresponding to Fe^{3+}/Fe^{2+} redox coupling was observed at 3.48 (that rise to 3.52 V) during oxidation and 3.35 V (reduced to 3.32 V) during reduction [37]. As shown in Fig. 8(d), the specific capacity remains more or less constant, suggestive of excellent capacity retention up to 50 cycles tested. The corresponding Columbic efficiency remains virtually constant at about 100% for 50 cycles, indicating the cyclic stability of the present PEGBCDMA based PEM in the half-cell tests, showing enhanced electrochemical stability relative to the PEGDA counterpart.

4. Conclusions

In this article, polyethylene glycol-*bis*-carbamate dimethacrylate (PEGBCDMA) has been successfully synthesized to afford solvent-free, non-flammable solid polymer electrolyte membranes for lithium-ion batteries. The PEGBCDMA film has shown to possess superior tensile strength and extensibility as compared to the PEGDA matrix. More importantly, high room temperature ionic conductivity at the level of superionic conductors (i.e., 10^{-3} S/cm) was achieved with the present PEM composed of 10/45/45 PEGBCDA/SCN/LiTFSI. Moreover, it exhibits an impressive level of 10^{-2} S/cm at an elevated temperature of 120 °**C**, which is comparable to organic liquid electrolyte, but with superior thermal stability. Of particular importance is that excellent capacity retention has been achieved with both $Li_4Ti_5O_{12}$/PEM/Li and $LiFePO_4$/PEM/Li half-cells, which exceeds those of the PEGDA system. In a nutshell, we have demonstrated the achievement of a new class of solid-state polymer electrolyte membrane for lithium-ion batteries.

Acknowledgment

Support of this work by NSF-DMR 1502543 is gratefully acknowledged.

Appendix A. Supplementary data

Supplementary data related to this article can be found at http://dx.doi.org/10.1016/j.jpowsour.2017.05.097.

References

[1] J.-M. Tarascon, M. Armand, Nature 414 (2001) 359–367.
[2] C.L. Schmidt, P.M. Skarstad, J. Power Sources 97 (2001) 742–746.
[3] J. Tollefson, Nature 456 (2008) 436.
[4] L. Lu, X. Han, J. Li, J. Hua, M. Ouyang, J. Power Sources 226 (2013) 272–288.
[5] K. Xu, Chem. Rev. 104 (2004) 4303–4418.
[6] U. von Sacken, E. Nodwell, A. Sundler, J. Dahn, Solid State Ionics 69 (1994) 284–290.
[7] Y. Chen, J.W. Evans, J. Electrochem. Soc. 143 (1996) 2708–2712.
[8] Q. Wang, W.-L. Song, L. Wang, Y. Song, Q. Shi, L.-Z. Fan, Electrochim. Acta 132 (2014) 538–544.
[9] Q. Wang, W.-L. Song, L.-Z. Fan, Q. Shi, J. Power Sources 279 (2015) 405–412.
[10] D. Fenton, J. Parker, P. Wright, Polymer 14 (1973) 589.
[11] P.V. Wright, Br. Polym. J 7 (1975) 319–327.
[12] S. Long, D. MacFarlane, M. Forsyth, Solid State Ionics 161 (2003) 105–112.
[13] P.J. Alarco, Y. Abu-Lebdeh, A. Abouimrane, M. Armand, Nat. Mat. 3 (2004) 476–481.
[14] M. Patel, A.J. Bhattacharyya, Ener. Environ. Sci. 4 (2011) 429–432.
[15] L.Z. Fan, Y.S. Hu, A.J. Bhattacharyya, J. Maier, Adv. Funct. Mater. 17 (2007) 2800–2807.
[16] M. Echeverri, N. Kim, T. Kyu, Macromolecules 45 (2012) 6068–6077.
[17] C. Gerbaldi, J.R. Nair, S. Ahmad, G. Meligrana, R. Bongiovanni, S. Bodoardo, N. Penazzi, J. Power Sources 195 (2010) 1706–1713.
[18] H.-J. Ha, Y.H. Kwon, J.Y. Kim, S.-Y. Lee, Electrochim. Acta 57 (2011) 40–45.
[19] M. Echeverri, C. Hamad, T. Kyu, Solid State Ionics 254 (2014) 92–100.
[20] M. Singh, O. Odusanya, G.M. Wilmes, H.B. Eitouni, E.D. Gomez, A.J. Patel, V.L. Chen, M.J. Park, P. Fragouli, H. Iatrou, Macromolecules 40 (2007) 4578–4585.
[21] C. Monroe, J. Newman, J. Electrochem. Soc. 150 (2003) A1377–A1384.
[22] C. Monroe, J. Newman, J. Electrochem. Soc. 152 (2005) A396–A404.
[23] L. Maisonneuve, O.a. Lamarzelle, E. Rix, E. Grau, H. Cramail, Chem. Rev. 115 (2015) 12407–12439.
[24] D.M. Lincoln, R.A. Vaia, Z.-G. Wang, B.S. Hsiao, R. Krishnamoorti, Polymer 42 (2001) 09975–09985.
[25] P. Badrinarayanan, W. Zheng, Q. Li, S.L. Simon, J. Non-Cryst. Solids 353 (2007) 2603–2612.
[26] S.D. Druger, M.A. Ratner, A. Nitzan, Solid State Ionics 9 (1983) 1115–1120.
[27] C. Berthier, W. Gorecki, M. Minier, M. Armand, J. Chabagno, P. Rigaud, Solid State Ionics 11 (1983) 91–95.
[28] L. Ning, W. De-Ning, Y. Sheng-Kang, Macromolecules 30 (1997) 4405–4409.

[29] S. Zhang, Z. Ren, S. He, Y. Zhu, C. Zhu, Spectrochim. Acta, Part A Mol. Biomol. Spectrosc. 66 (2007) 188–193.
[30] K. Kato, T. Matsui, S. Tanaka, Appl. Spectrosc. 41 (1987) 861–865.
[31] X. Wang, M.D. Soucek, Prog. Org. Coat. 76 (2013) 1057–1067.
[32] M.T. Lemon, M.S. Jones, J.W. Stansbury, J. Biomed. Mat. Res. Part A 83 (2007) 734–746.
[33] J. Kim, J. Cho, Electrochem. Solid-State Lett. 10 (2007) A81–A84.
[34] Z. Yang, D. Choi, S. Kerisit, K.M. Rosso, D. Wang, J. Zhang, G. Graff, J. Liu, J. Power Sources 192 (2009) 588–598.
[35] R. He, M. Echeverri, D. Ward, Y. Zhu, T. Kyu, J. Membr. Sci. 498 (2016) 208–217.
[36] J. Cao, R. He, T. Kyu, Curr. Opin. Chem. Eng. 15 (2017) 68–75.
[37] R. Dominko, M. Bele, M. Gaberscek, M. Remskar, D. Hanzel, S. Pejovnik, J. Jamnik, J. Electrochem. Soc. 152 (2005) A607–A610.